ACS APPLIED MATERIALS & INTERFACES

Research Article

www.acsami.org

Antibacterial Coatings on Titanium Surfaces: A Comparison Study Between *in Vitro* Single-Species and Multispecies Biofilm

Maria Godoy-Gallardo,[†,‡,§] Zhejun Wang,[#,∥] Ya Shen,[#] José M. Manero,[†,‡,§] Francisco J. Gil,[†,‡,§] Daniel Rodriguez,*[,†,‡,§] and Markus Haapasalo[#]

[†]Biomaterials, Biomechanics and Tissue Engineering Group, Department of Materials Science and Metallurgy, Technical University of Catalonia (UPC), ETSEIB, Av. Diagonal 647, 08028, Barcelona, Spain

[‡]Bioingeniería, Biomateriales y Nanomedicina (CIBER-BBN), C/Monforte de Lemos 3-5, Pabellón 11, 28029 Madrid, Spain

[§]Centre for Research in NanoEngineering (CRNE)-UPC, C/Pascual i Vila 15, 08028, Barcelona, Spain

[#]Division of Endodontics, Department of Oral Biological and Medical Sciences, University of British Columbia, Vancouver, British Columbia V6T 1Z3, Canada

[∥]The State Key Laboratory Breeding Base of Basic Science of Stomatology (Hubei-MOST) and Key Laboratory of Oral Biomedicine Ministry of Education, School and Hospital of Stomatology, Wuhan University, 237 Luoyu Road, Wuhan, Hubei 430079, PR China

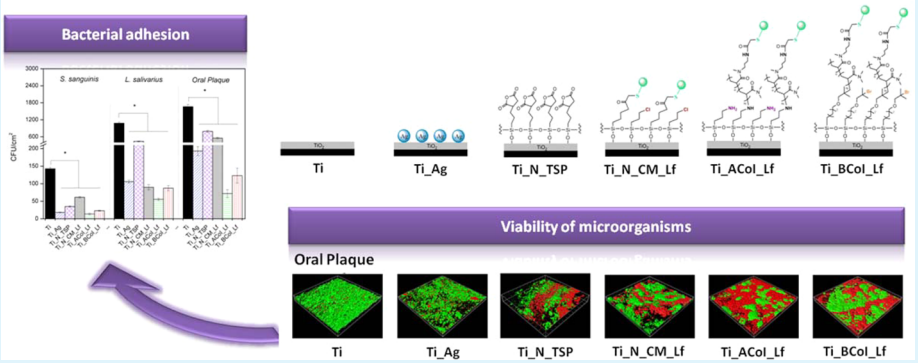

ABSTRACT: Dental plaque is a biofilm that causes dental caries, gingivitis, and periodontitis. Most of the studies in antibacterial coatings have been conducted by *in vitro* single-species biofilm formation, but oral biofilm involves more than 700 different bacterial species that are able to interact. Therefore, new studies are focused on *in vitro* multispecies biofilm models that mimic *in vivo* biofilms. The aim of the present work was to study different antibacterial coatings onto titanium surfaces and evaluate the *in vitro* antimicrobial properties of the surfaces on two different bacterial species and an oral biofilm. The lactate dehydrogenase assay determined that treated samples did not affect fibroblast viability. In addition, the viability of microorganisms on modified samples was evaluated by a LIVE/DEAD BacLight bacterial viability kit. Although a decrease in viable bacteria onto treated samples was obtained, the results showed differences in effectiveness when single-biofilm and oral plaque were tested. It confirms, as we expected, the distinct sensitivities that bacterial strains have. Thus, this multispecies biofilms model holds a great potential to assess antibacterial properties onto samples for dental purposes.

KEYWORDS: *single biofilm, multispecies biofilm, antibacterial coatings, titanium, hLf1-11 immobilization, silver electrodeposition, TESPSA silanization*

1. INTRODUCTION

Peri-implantitis is a disease which appears when dental plaque induces inflammation of the peri-implant tissue, and it is associated with bone loss.[1,2] Implant plaque consists of an oral biofilm initiated by free-floating bacterial cells attaching to the implant surface. Then, the microorganisms grow into mature, structurally complex biofilm where some bacteria detach into the oral environment.

Most of the studies in antibacterial implant coatings have been conducted by *in vitro* single-species biofilm formation, although oral biofilm involves more than 700 different interacting bacterial species.[3−5] The bacterial complexity of dental plaque is divided into two groups regarding their effect in biofilm formation: primary and late colonizers. Primary colonizers consist mainly of *Streptococcus* genus (such as *Streptococcus sanguinis*) and display higher adherence capabilities compared to other bacterial species.[6,7] Other primary colonizers are *Actinomyces*, *Veillonella*, and *Haemophilus* genera.[8−10] The late colonizers include bacteria such as *Prevotella intermedia*, *Treponema denticola*, *Aggregatibacter*

Received: January 14, 2015
Accepted: March 3, 2015
Published: March 3, 2015

DOI: 10.1021/acsami.5b00402
ACS Appl. Mater. Interfaces 2015, 7, 5992−6001

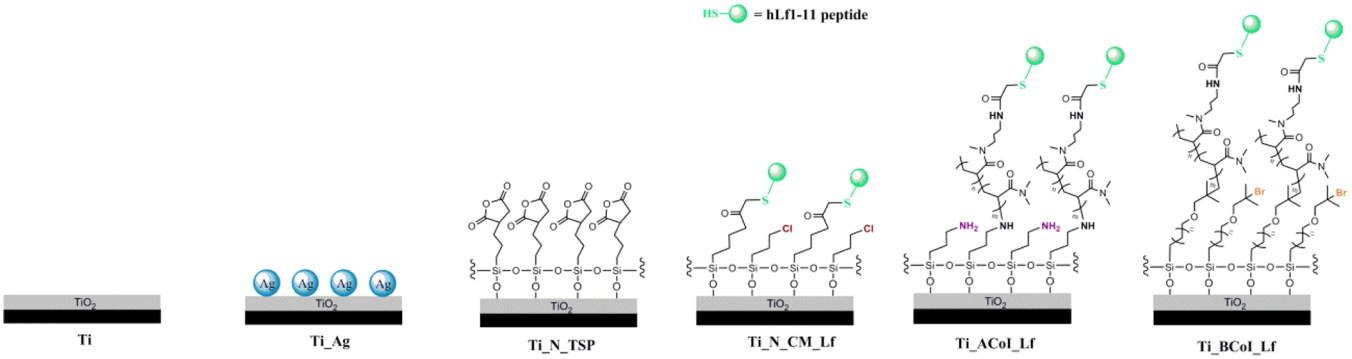

Figure 1. Schematic representation of the applied surface treatments.

actinomycetemcomitans, *Tannerella forsythia*, and *Porphyromonas gingivalis*.[8−10] In particular, *Lactobacillus salivarius* interacts with other colonizers, and their metabolic products are necessary for the biofilm formation and maintenance.[11] Therefore, the development of new *in vitro* multispecies biofilm models should seek to better mimic the characteristics of *in vivo* biofilms.

On the basis of these premises, a new *in vitro* multispecies biofilm model has been proposed[12−14] in order to evaluate the efficacy of antibacterial conditions. For that purpose, confocal laser scanning microscopy (CLSM) has been considered as the most useful technique for three-dimensional reconstruction, identification of viable bacteria, and comparison of biofilm modifications under different agents.

Titanium is the material of choice for dental implants because of its mechanical properties and the capability of osseointegration. However, several challenges must be overcome to provide titanium devices with antibacterial properties. One strategy to prevent infections is the deposition of antibacterial agents on titanium surfaces. Specifically, silver has been shown to be effective as a broad-spectrum antibacterial material, even against drug-resistant strains.[15,16] Different techniques have been used to incorporate silver onto the surface of biomaterials such as electrodeposition,[17] chemical vapor deposition,[18] and magnetron cosputtering.[19] Other methods are based in the titanium surface modification by using self-assembled monolayers (SAMs) which could serve as an initiator for further biomolecules immobilization.[20−22] The type of biomolecule depends on the appropriate terminal functional group in the monolayer, e.g., alkanethiols, disulfides, trichlorosilanes, trimethoxysilanes, organosilicon hydrides, phosphoric acids, and phosphates.[23] In the case of silanization, a silane can create a covalent bond with the hydroxyl groups present on metal surfaces (e.g., titanium) and fix the hydroxylsilane onto the substrate.[24] Moreover, they are able to covalently immobilize biomolecules (e.g., an antimicrobial peptides) to promote specific cells responses.[25] Antimicrobial peptides (AMP) have recently attracted much attention due to their strong antibacterial activity against a broad spectrum of microorganisms and low rates of bacterial resistance.[20,26−29] Their activity is due to their capacity to target and disrupt bacterial membranes.[26,30,31] Although AMPs vary in sequence and structure, all of them adopt an amphipathic structure which interact with phospholipids of the bacteria membrane and increase its permeability, which is destructive for the bacteria.[26,32] An example is the peptide hLf1-11, the 1-11 amino acid segment sequence of human lactoferrin, which is able to destabilize the plasma membrane of the bacteria by depolarization and iron-binding.[33,34]

Alternatively, biomaterial surfaces may be functionalized by grafting of polymer brushes by atom transfer radical polymerization (ATRP). Polymer brushes consist of an assembly of polymer chains which are in contact with the surface substrate by one terminal end. Moreover, ATRP enhances the efficiency of peptide immobilization due to an increase in the spatial density of a diverse number of functional groups on the surface. This work has two main goals: (1) to investigate the efficiency of five antibacterial coatings on titanium (silver electrodeposition, TESPSA silane coating, hLf1-11 peptide binding with 3-chloropropyl triethoxysilane (CPTES) silane, and ATRP peptide binding with two different chemical routes); (2) to compare the antibacterial properties of these coatings on single species and multispecies oral biofilms.

2. MATERIALS AND METHODS

2.1. Sample Preparation. Titanium (c.p grade 2) disks (10 mm diameter, 2 mm thickness) were smoothed up to a surface roughness (R_a) under 40 nm. Once polished, samples were cleaned with isopropanol, ethanol, water, and acetone for 15 min each by sonication.

2.2. Surface Treatment Procedures. *2.2.1. Silver Electrodeposition.* The silver electrodeposition process was controlled with a Potentiostat (PARSTAT 2273, Princeton Applied Research, Oak Ridge, TN, USA) and applied as previously explained.[17] Briefly, a potential with a rectangular pulse shape (EI = 0 V, EF = 5 V, ST = 500 ms, SH = 10 mV, PW = 100 ms) was applied to the working electrode, with a full-cycle period of 25 s. The electrolyte consisted of 0.1 M $AgNO_3$ and 0.2 M $Na_2S_2O_3$, whereas the time of each process was 500 cycles. The new surface was performed on the abutment, while the implant remained untreated. After treatment, all samples were sonicated in ethanol, distilled water, and acetone for 15 min each.

2.2.2. TESPSA Silanization. Titanium surfaces were activated with 5 M NaOH for 24 h at 60 °C.[35] Subsequently, samples were cleaned by immersion in distilled water for 30 min twice, washed with acetone, and dried with nitrogen gas. Pretreated titanium samples were silanized with TESPSA (0.5%, v/v) in anhydrous toluene for 1 h at 70 °C in a nitrogen atmosphere. The silanization was applied in dissolution of 3% (v/v) *N*,*N*-diisopropylethylamine (DIEA) to maintain a basic environment. Once the reaction was completed, samples were sonicated with distilled water for 10 min, washed with isopropanol, ethanol, distilled water, and acetone, and dried with nitrogen.

2.2.3. Immobilization of hLf1-11 Peptide onto Titanium Samples by CPTES Silanization. The immobilization of the hLf1-11 peptide on titanium surfaces has been previously described by Godoy-Gallardo et al.[20] as an adaptation from other protocols.[28,36,37] Briefly, surfaces were activated by alkaline etching and then silanized with CPTES (2.0%, v/v) in anhydrous toluene. Then, a cross-linker (maleimide acid *N*-

DOI: 10.1021/acsami.5b00402
ACS Appl. Mater. Interfaces 2015, 7, 5992−6001

hydroxysuccinimide ester) was added to the silanized surfaces, and finally, the hLf1-11 peptide was immobilized by overnight immersion (200 μM solution of hLf1-11 dissolved in 0.5 mg/mL Na_2CO_3). Surfaces were washed with PBS and dried with nitrogen.

2.2.4. Immobilization of hLf1-11 Peptide onto Titanium Samples by Atom Transfer Radical Polymerization (ATRP). This process corresponds to protocols published by Gao et al.[38,39] and Godoy-Gallardo et al.[40] Concisely, titanium surfaces were activated with oxygen plasma treatment (Standard Plasma System Femto, Diener electronic GmbH, Germany) at a power of 100 W for 10 min. The first group of samples (Ti_ACoI_Lf) was silanized with 3-Triethoxysilylpropylamine (APTES), and the amino group was activated prior to the ATRP process.[40] The second group of samples (Ti_BCoI_Lf) was immersed overnight in a solution of 11-(2-bromo-2-methyl) propionyloxyundecenyltrichlorosilane (BPTCS) in toluene at room temperature (the synthesis of BPTCS was detailed by Matyjaszewski et al.[41]). Samples were cleaned and dried with nitrogen.

Afterward, ATRP was performed for all samples by the copolymerization of DMA-APMA followed by overnight incubation in a solution of hLf1-11 (1 mg/mL) in PBS (pH 8.5) at room temperature. Remaining activated groups were capped by immersion in 2-mercaptoethanol for 24 h, and samples were sonicated with PBS and dried with nitrogen.

The treated samples (Figure 1) and their controls were codified as follows.

Ti: smooth titanium

Ti_Ag: titanium + silver electrodeposition

Ti_N_TSP: titanium + TESPSA

Ti_N_CM_Lf: titanium + CPTES + maleimide cross-linker + hLf1-11 peptide

Ti_ACoI_Lf: titanium + APTES + DMA-APMA copolymer + iodoacetyl cross-linker + hLf1-11 peptide

Ti_BCoI_Lf: titanium + BPTCS + DMA-APMA copolymer + iodoacetyl cross-linker + hLf1-11 peptide

2.3. Physicochemical Characterization of the Surfaces. *2.3.1. Morphological Analysis.* Scanning electron microscopy (Zeiss Neon40 FE-SEM, Carl Zeiss NTS GmbH, Germany) was used to observe the surface morphology of the samples. Five images were taken for each surface at a working distance of 7 mm and a potential of 5 kV.

2.3.2. Contact Angle Analysis. Static water contact angles were measured with distilled water (Millipore Milli-Q, Merck Millipore Corporation, USA) using the sessile drop method (Contact Angle System OCA15 plus; Dataphysics, Germany). Measurements were acquired in triplicate for three samples in each series at room temperature, with a volume of 3 μL and a dose rate of 1 μL/min.

Surface energy was also calculated with the Owens, Wendt, Rabel, and Kaelble (OWRK) equation applied to both water and diiodomethane measurements, as previously explained.[20,40] Data was interpreted with SCA 20 software (Dataphysics).

2.3.3. Roughness Analysis. White light interferometry (Wyko NT1100, Veeco Instruments, USA) was used to measure the surface topography of the samples by a 5× objective lens and an area of 736 × 480 μm. Three measurements were collected at different positions on three samples of each group. The arithmetic average height (R_a), the surface skewness (R_{sk}), and the surface kurtosis (R_{ku}) were studied.[42,43] Data analysis was performed with Wyko Vision 232 software (Veeco Instruments).

2.3.4. X-ray Photoelectron Spectroscopy Analysis. The chemical composition of the surfaces was analyzed by X-ray photoelectron spectroscopy (XPS). Measurements were performed using an XR50 Mg anode source operating at 150 W and a Phoibos 150 MCD-9 detector (D8 advance, SPECS Surface Nano Analysis GmbH, Germany).

High resolution spectra were collected using 25 eV at 0.1 eV steps with a chamber pressure below 7.5×10^{-9} mbar. Binding energies were calibrated using the C 1s signal at 480 eV. Two specimens were analyzed for each studied condition.

2.4. Biological Characterization of the Surfaces. *2.4.1. Cell Culture of Human Foreskin Fibroblasts (HFFs).* Details of the cell culture assays were previously described elsewhere.[17,20,40] HFFs cells were grown and maintained in supplemented DMEM. Cells were cultured in 75 cm^2 cell culture flasks at 37 °C, and the medium was refreshed every 2 days. HFFs were detached by trypsinization, centrifuged for 5 min at 300*g*, resuspended in fresh DMEM medium, and seeded. Cells between passage three and eight were used in all experiments.

2.4.1.1. Cell Cytotoxicity Assay. Indirect *in vitro* cytotoxicity tests of the treated surfaces of HFFs cells were carried out by analyzing the activity of the lactate dehydrogenase (LDH) enzyme by the Cytotoxicity Detection Kit LDH. Each specimen was immersed in DMEM for 72 h at 37 ± 2 °C with an extraction medium area/volume ratio of 0.5 cm^2/1 mL (according to ISO 10993-5). Afterward, the extraction medium was removed and diluted with DMEM (dilution 1/0; 1/1; 1/10; 1/100; 1/1000).[40]

HFFs were seeded at 5000 cells/mL in a 96-well plate and allowed to adhere for 24 h at 37 °C. Then, the medium was aspired, substituted by the extracts, and incubated for another 24 h. The release of LDH was determined by measuring the optical density of 490 nm by an ELx800 Universal Microplate Reader (Bio-Tek Instruments, Inc. Winooski, VT, USA).

2.4.1.2. Cell Proliferation Assay. Additionally, the cell proliferation rate was assessed by the Cytotoxicity Detection Kit LDH assay. A quantity of 5000 cells was seeded on modified surfaces placed in 48-well plates and evaluated at 4, 24, 72, and 168 h of incubation with complete medium. Afterward, cells were lysed with 200 μL/well of M-PER, and the release of LDH was measured, as explained in the cell cytotoxicity assay.

2.4.2. Antimicrobial Properties of the Treated Surfaces. The bacterial assays were carried out by following protocols reported in the literature to evaluate the efficiency of antibacterial coatings.[20,40] The strains used in the study were *Streptococcus sanguinis* (CECT 480, Colección Española de Cultivos Tipo (CECT), Valencia, Spain) and *Lactobacillus salivarius* (CCUG 17826, Culture Collection University of Göteborg (CCUG), Göteborg, Sweden). Moreover, the oral plaque collected from one volunteer was also used. The Human Research Ethics Committee of the University of British Columbia (permission H12-02430) approved this experiment. *S. sanguinis* was grown and maintained on Todd-Hewitt (TH) broth (Scharlau Todd-Hewitt broth, Scharlab SL, Sentmenat, Spain), *L. salivarius* on MRS broth (Scharlau MRS broth, Scharlab SL), and oral plaque on Heart Infusion Broth (BHI) (Difco, Detroit, MI, USA). For monospecies biofilm, the bacteria suspensions were incubated overnight at 37 °C in air before each assay and the optical density was adjusted to 0.2 ± 0.01 at 600 nm (about 1×10^8 colony forming units (CFU)/mL). For the oral plaque, the optical density was adjusted to 0.1 at 405 nm and then diluted 1:10.[12,13] All assays were performed in static conditions, and three replicates for each condition were used.

2.4.2.1. Bacterial Adhesion on Titanium Surfaces. As described by Godoy-Gallardo et al.,[20,40] modified samples were incubated with 1 mL of the proper bacterial suspension solution for 2 h at 37 °C. Afterward, the suspension was aspired and disks were rinsed twice with PBS. Then, bacteria were detached from the titanium surface by vortexing in 1 mL of PBS for 5 min.[17,20,40] These bacteria were diluted and seeded on TH agar for *S. sanguinis*, MRS agar plates for *L. salivarius*, and Tryptic Soy Agar for oral plaque. CFU plate counting was performed after 24 h of incubation at 37 °C and expressed as adhered CFU/cm^2.

2.4.2.2. Viability of Bacteria on Modified Samples. The measure of bacteria viability was adapted from protocols previously reported by Godoy-Gallardo[40] and Shen et al.[12−14] Biofilm formation was assessed with the LIVE/DEAD BacLight bacterial viability kit (Life Technologies, Carlsbad, CA, USA). One milliliter of bacterial suspension (1×10^8 cells/mL, ABS 0.2 ± 0.01 at 600 nm) was seeded onto titanium surfaces and incubated at 37 °C for 1, 2, 3, and 4 weeks in anaerobic conditions. After incubation, samples were washed twice with PBS and transferred into a 48-well microtiter plate (Nunc, Thermo Scientific, Waltham, MA, USA). Adherent bacteria were

DOI: 10.1021/acsami.5b00402
ACS Appl. Mater. Interfaces 2015, 7, 5992−6001

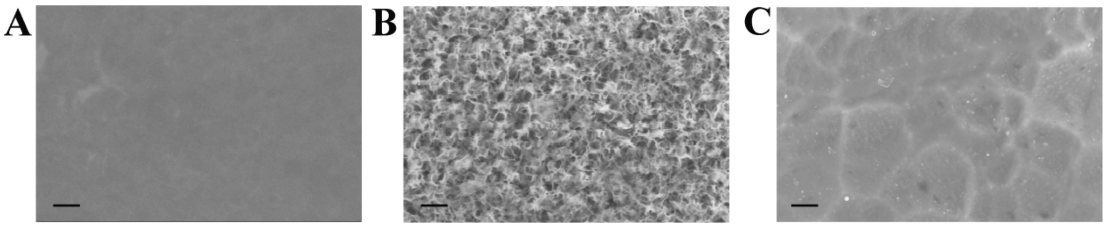

Figure 2. SEM images of (A) smooth titanium (Ti) and samples activated by plasma (Ti_ACoI_Lf and Ti_BCoI_Lf); (B) titanium activated with NaOH pretreatment (Ti_N_TSP and T_N_CM_Lf); (C) silver electrodeposition (Ti_Ag) (Scale: 300 nm).

Table 1. Values (Mean ± Standard Deviation) of Contact Angle (CA), Surface Free Energy (SFE), with Dispersive (DISP) and Polar (POL) Components, for Each Surface Treatment

	CA (deg)	SFE (mJ/m^2)	DISP (mJ/m^2)	POL (mJ/m^2)
Ti	68.7 ± 2.7	47.5 ± 2.4	39.4 ± 2.2	8.1 ± 1.2
Ti_Ag	64.1 ± 2.9[a]	51.9 ± 2.3[a]	42.5 ± 2.4	9.4 ± 1.5
Ti_N_TSP	31.2 ± 4.6[a]	71.8 ± 2.1[a]	47.3 ± 1.1[a]	24.5 ± 2.2[a]
Ti_N_CM_Lf	51.6 ± 9.9[a]	60.2 ± 5.4[a]	45.2 ± 1.5[a]	15.0 ± 5.2[a]
Ti_ACoI_Lf	64.6 ± 2.7[a]	47.0 ± 1.8	35.5 ± 1.3[a]	11.5 ± 1.5[a]
Ti_BCoI_Lf	72.1 ± 5.0[a]	46.3 ± 2.3	37.4 ± 6.6	6.6 ± 2.6[a]

[a]Statistically significant difference versus control Ti ($P < 0.05$).

stained by incubation with 50 μL of a dye-solution (1.5 μL of SYTO and 1.5 μL of propidium iodide/1 mL of NaCl buffer (0.85%)) for 15 min. Dyed surfaces were analyzed by confocal laser scanning microscopy CLSM images with a 20× lens. Images were acquired with the software EZ-C1 (EZ-C1 v3.40, build 691, Nikon, NY, USA) at five random positions of the surfaces, and a stack of 40 slices (1 μm thick each) was scanned. Image stacks were analyzed by Imaris software (Bitplane, Zurich, Switzerland) in order to evaluate the volume ratio of dead cells.

2.5. Statistical Analysis. All data were analyzed by a non-parametric U Mann−Whitney test (IBM SPSS Statistics 20 software, Armonk, NY, USA). Statistical significance was set at a P value <0.05.

3. RESULTS

3.1. Morphological Analysis. As shown in Figure 2A, plasma activation, subsequent brush polymerization, and finally hLf1-11 conjugation (Ti_ACoI_Lf and Ti_BCoI_Lf) did not alter the morphology of the sample in comparison with control titanium (Ti). However, sodium hydroxide treatment resulted in noticeable differences in morphology (Ti_N_TSP and Ti_N_CM_Lf, Figure 2B). NaOH treated samples revealed a layer of micropore structure[35] (less than 1 μm in diameter) of sodium titanate.[44] Likewise, silver electrodeposition treatment exposed round etchings and globular deposits which had a homogeneously distribution onto the titanium surfaces. These deposits, even after intense sonication, remained on the surface.

3.2. Contact Angle Analysis. In order to establish the surface hydrophobicity at a microscopic scale, contact angle and surface energy were evaluated (Table 1). TESPSA and lactoferrin peptide immobilization by silanization (Ti_N_TSP and Ti_N_CM_Lf) onto surfaces decrease contact angle values with a significant increment of the SFE. In contrast, silver deposition and covalent immobilization of hLf1-11 on polymerized substrates (Ti_ACoI_Lf and Ti_BCoI_Lf) increased CA values in comparison with its control (data not shown). An increase in the polar component of the SFE of these samples was also observed. The modifications of the SFE were mostly due to changes in its polar component since the dispersive part remained fairly constant. Comparing rates of peptide attachment, the surface wettability was higher when the modification was carried out by polymerization than via silanization.

3.3. Roughness Analysis. The roughness was represented by three different parameters (R_a, R_{ku}, and R_{sk}) (Table 2).

Table 2. Roughness Values (Mean ± Standard Deviation) for Each Surface Treatment

	R_a (nm)	R_{ku} (nm)	R_{sk} (nm)
Ti	25.1 ± 5.4	4.1 ± 1.8	0.8 ± 0.6
Ti_Ag	76.0 ± 7.0[a]	11.0 ± 6.0	1.0 ± 0.8
Ti_N_TSP	96.9 ± 6.2[a]	7.5 ± 2.6	0.4 ± 0.8
Ti_N_CM_Lf	95.0 ± 30.5[a]	4.0 ± 1.1	2.6 ± 1.1[a]
Ti_ACoI_Lf	30.5 ± 3.1	6.1 ± 2.0	1.9 ± 1.0[a]
Ti_BCoI_Lf	30.4 ± 3.5	7.1 ± 1.7	2.0 ± 1.3[a]

[a]Statistically significant difference versus control Ti ($P < 0.05$).

Pretreated samples with NaOH etching (Ti_N_TSP and Ti_N_CM_Lf) showed a statistically significant increase in roughness in comparison with control sample (Ti). Similarly, silver electrodeposition influenced the roughness of the Ti surfaces. In contrast, atom transfer radical polymerization treatment did not result in significant differences in surface roughness. Both R_{ku} and R_{sk} parameters displayed higher values in almost all conditions in comparison with control titanium.

3.4. Chemical Composition by X-ray Photoelectron Spectroscopy. The atomic composition of all surfaces was studied by means of XPS (Table 3). For all the conditions, an increase in the percentage of C 1s and N 1s was observed. A reduction in Ti 2p signal in comparison with control titanium was measured in all samples, but a decrease in the O 1s signal was detected only in samples treated with either the CPTES or ATRP method.

Silver electrodeposition was easily characterized by the presence of silver on the substrate (2.8% for Ti_Ag) and silanization by the presence of silicon (6.9% for Ti_N_TSP, 1.6% for Ti_N_CM_Lf, 1.0% for Ti_ACoI_Lf, and 1.7% for Ti_BCoI_Lf). Sulfur was also detected on electrodeposited surfaces (1.5% for Ti_Ag) as well as on peptide-conjugated surfaces (0.9% for Ti_N_CM_Lf, 1.3% for Ti_ACoI_Lf, and

DOI: 10.1021/acsami.5b00402
ACS Appl. Mater. Interfaces 2015, 7, 5992−6001

Table 3. Chemical Composition (at %) and Si/Ti, S/Ti, and Ag/Ti Relative Atomic Ratios

	C 1s %	N 1s %	O 1s %	S 2p %	Si 2p %	Ti 2p %	Ag 3d %	S/Ti	Si/Ti	Ag/Ti
Ti	36.3 ± 7.3	2.3 ± 1.6	47.9 ± 6.4	0.2 ± 0.1	1.1 ± 0.7	13.2 ± 3.3	*a*	0.01 ± 0.01	0.1 ± 0.8	*a*
Ti_Ag	46.0 ± 9.7	1.0 ± 0.4	42.9 ± 5.3	1.5 ± 0.6	*a*	5.8 ± 4.2	2.8 ± 0.9	0.2 ± 0.2	*a*	0.6 ± 0.3
Ti_N_TSP	41.2 ± 9.0	0.7 ± 0.2	42.7 ± 6.5	*a*	6.9 ± 1.6	8.4 ± 4.1	*a*	*a*	1.0 ± 0.5	*a*
Ti_N_CM_Lf	57.4 ± 2.5	11.5 ± 2.4	26.0 ± 1.5	0.9 ± 0.2	1.6 ± 0.4	2.6 ± 1.0	*a*	0.4 ± 0.1	0.6 ± 0.07	*a*
Ti_ACoI_Lf	58.6 ± 1.7	13.1 ± 6.8	23.9 ± 7.4	1.3 ± 0.4	1.0 ± 0.1	1.6 ± 0.8	*a*	1.3 ± 0.4	0.7 ± 0.3	*a*
Ti_BCoI_Lf	71.8 ± 1.0	12.1 ± 1.5	13.7 ± 0.1	0.9 ± 0.02	0.7 ± 0.1	0.8 ± 0.1	*a*	1.1 ± 0.2	0.8 ± 0.04	*a*

[a]Lower than the detection limit.

0.9% for Ti_BCoI_Lf). The S/Ti ratio indicated that ATRP facilitated peptide attachment compared to silanization (S/Ti ratio of 0.4 for Ti_AI_Lf, 1.3 for Ti_ACoI_Lf, and 1.1 for Ti_BCoI_Lf).

3.5. Cell Cytotoxicity Assay. Comparisons between the 6 test groups at 1 day incubation for different concentrations of cell culture extract are summarized in Figure 3. After 24 h, the viability of cells exposed to treated samples was not significantly different compared to control titanium (Ti). Thus, all modified samples had a low or noncytotoxic effect.

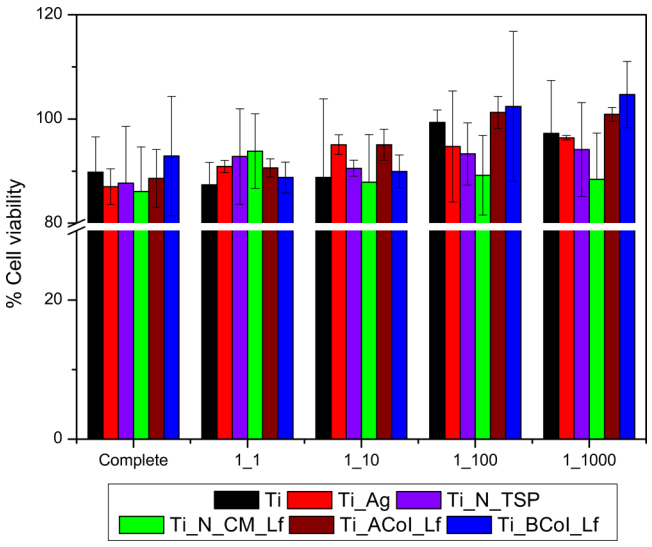

Figure 3. Cytotoxicity of HFFs on titanium surfaces after a 1 day incubation.

3.6. Cell Proliferation Assay. For all test groups, the proliferation of HFFs over 4 h and 1, 3, and 7 days of incubation was measured (Figure 4). For 4 h and 1 d of culture, samples covered by ATRP strategy showed a lower number of viable cells than untreated titanium. However, no significant differences in cell proliferation were observed between treated samples and control ones.

3.7. Bacterial Adhesion on Titanium Surfaces Assay. Results of bacteria assay for *S. sanguinis*, *L. salivarius*, and oral plaque after 2 h of incubation on treated samples and control titanium are shown in Figure 5. All modified samples significantly reduced the adhesion of all bacteria suspensions, with the highest reduction measured for *S. sanguinis*. Moreover, the samples with hLf1-11 peptide attached by ATRP polymerization (Ti_ACoI_Lf and Ti_BCoI_Lf) showed the highest reduction.

3.8. Viability of Microorganisms on Modified Samples. Results of live bacteria on modified surfaces and control titanium after 1, 2, 3, and 4 weeks of incubation are shown in Figure 6. Overall, all treated surfaces drastically reduced the number of viable bacteria of both strains and the oral plaque. Control titanium surfaces showed no statistically significant differences on bacteria viability at different times for all three conditions. In particular, silver electrodeposition exhibited the highest antibacterial effect onto titanium surfaces (Ti_Ag). Noteworthy, single-species biofilm (*S. sanguinis* and *L. salivarius*) displayed a higher decrease in comparison with oral multispecies biofilm (oral plaque). Interestingly, an

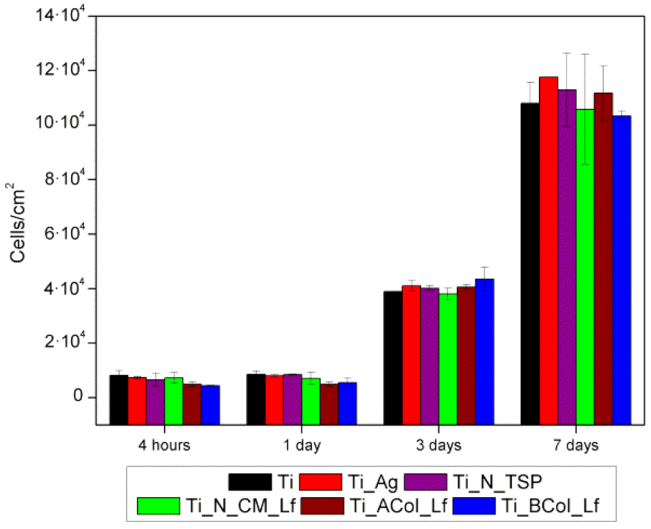

Figure 4. Proliferation of HFFs on the studied surfaces after 4 h and 1, 3, and 7 days of incubation measured by an LDH assay.

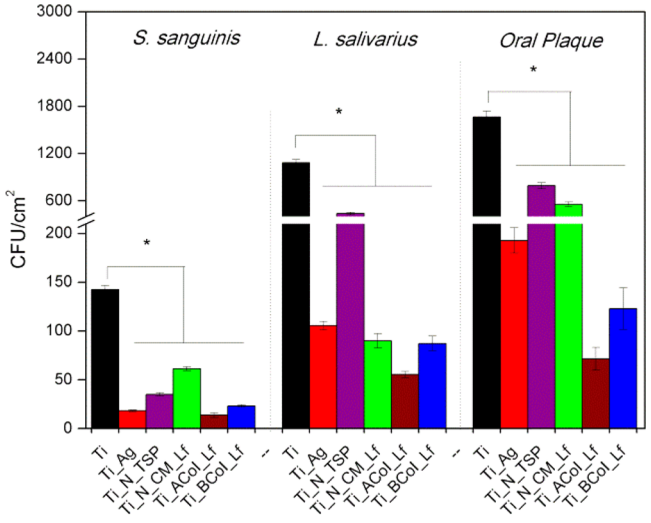

Figure 5. Bacterial adhesion of oral plaque, *S. sanguinis*, and *L. salivarius* on titanium surfaces after 2 h of incubation at 37 °C. Statistically significant differences are indicated with an "∗" ($P < 0.05$).

DOI: 10.1021/acsami.5b00402
ACS Appl. Mater. Interfaces 2015, 7, 5992−6001

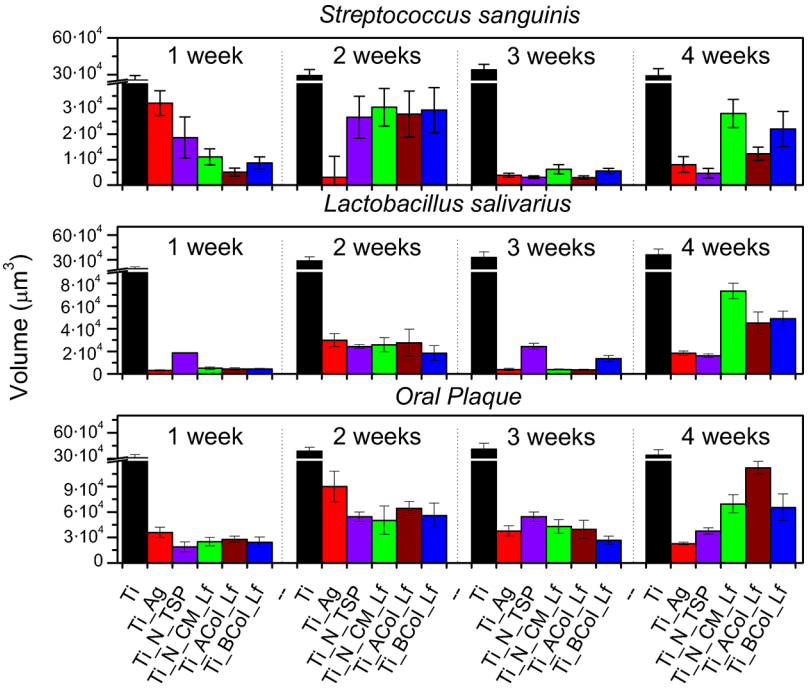

Figure 6. Live bacteria of *S. sanguinis*, *L. salivarius*, and oral plaque at different times of incubation at 37 °C.

Table 4. Ratio of Dead Bacteria [Red Cells/(Red Cells + Green Cells)] for 1 and 2 Weeks of Incubation at 37 °C

	1 week			2 weeks		
	S. sanguinis	*L. salivarius*	oral plaque	*S. sanguinis*	*L. salivarius*	oral plaque
Ti	0.001 ± 0.0	0.003 ± 0.002	0.001 ± 0.0	0.002 ± 0.003	0.04 ± 0.04	0.002 ± 0.002
Ti_Ag	0.1 ± 0.05	0.06 ± 0.04	0.1 ± 0.06	0.4 ± 0.2	0.3 ± 0.2	0.2 ± 0.1
Ti_N_TSP	0.1 ± 0.07	0.1 ± 0.08	0.1 ± 0.08	0.1 ± 0.05	0.2 ± 0.08	0.3 ± 0.06
Ti_N_CM_Lf	0.1 ± 0.05	0.1 ± 0.06	0.1 ± 0.06	0.4 ± 0.2	0.4 ± 0.2	0.2 ± 0.09
Ti_ACoI_Lf	0.1 ± 0.05	0.4 ± 0.2	0.1 ± 0.06	0.6 ± 0.3	0.4 ± 0.2	0.3 ± 0.2
Ti_BCoI_Lf	0.1 ± 0.04	0.3 ± 0.1	0.1 ± 0.07	0.4 ± 0.09	0.2 ± 0.07	0.4 ± 0.07
	3 weeks			4 weeks		
	S. sanguinis	*L. salivarius*	oral plaque	*S. sanguinis*	*L. salivarius*	oral plaque
Ti	0.04 ± 0.04	0.004 ± 0.01	0.02 ± 0.04	0.05 ± 0.05	0.03 ± 0.04	0.03 ± 0.03
Ti_Ag	0.5 ± 0.05	0.5 ± 0.08	0.3 ± 0.1	0.3 ± 0.08	0.3 ± 0.2	0.5 ± 0.1
Ti_N_TSP	0.1 ± 0.06	0.5 ± 0.1	0.4 ± 0.1	0.3 ± 0.07	0.4 ± 0.2	0.5 ± 0.1
Ti_N_CM_Lf	0.4 ± 0.08	0.4 ± 0.2	0.4 ± 0.2	0.3 ± 0.08	0.6 ± 0.2	0.3 ± 0.1
Ti_ACoI_Lf	0.4 ± 0.1	0.5 ± 0.1	0.5 ± 0.1	0.6 ± 0.2	0.5 ± 0.2	0.2 ± 0.1
Ti_BCoI_Lf	0.3 ± 0.1	0.5 ± 0.2	0.4 ± 0.2	0.6 ± 0.2	0.6 ± 0.2	0.3 ± 0.1

increase of the presence of live bacteria in treated samples was detected after the fourth week for all conditions, except for Ti_N_TSP and Ti_Ag samples with *L. salivarius* cultures.

The ratio of dead/live bacteria was measured (Table 4) to confirm the antibacterial properties of the treated surfaces. All treated samples exhibited a higher dead/live ratio than control titanium through all times of study. Moreover, during the first 2 weeks, no differences were detected among the three different biofilms. However, after 3 weeks, the dead/live ratio was lower when multispecies biofilm was used instead of a single strain biofilm.

Images of viable cells (green dots) and dead bacteria (red dots) obtained by CLSM are presented in Figure 7. Treated samples reduced the number of viable bacteria while dead bacteria were detected on the modified surfaces.

4. DISCUSSION

Reduction and control of dental plaque is an obvious issue in prevention and treatment of oral diseases. Various types of antimicrobial strategies have been suggested to reduce or avoid the effect of peri-implantitis on surrounding tissues. The suppression of bacteria adherence, the initial step in biofilm formation, could be a prophylactic measure against the formation of the oral plaque. The application of a surface treatment or coating on titanium is another preferred strategy.

As previously mentioned, silver is a widely used biocide with effects comparable to those of antibiotics but without the development of bacteria resistance.[45,46] The treatment analyzed in the present study consists of the electrochemical deposition of silver[17] with a low release of silver in the medium. It does not require the application of external agents, such as UV irradiation, to exert antibacterial effects.

DOI: 10.1021/acsami.5b00402
ACS Appl. Mater. Interfaces 2015, 7, 5992−6001

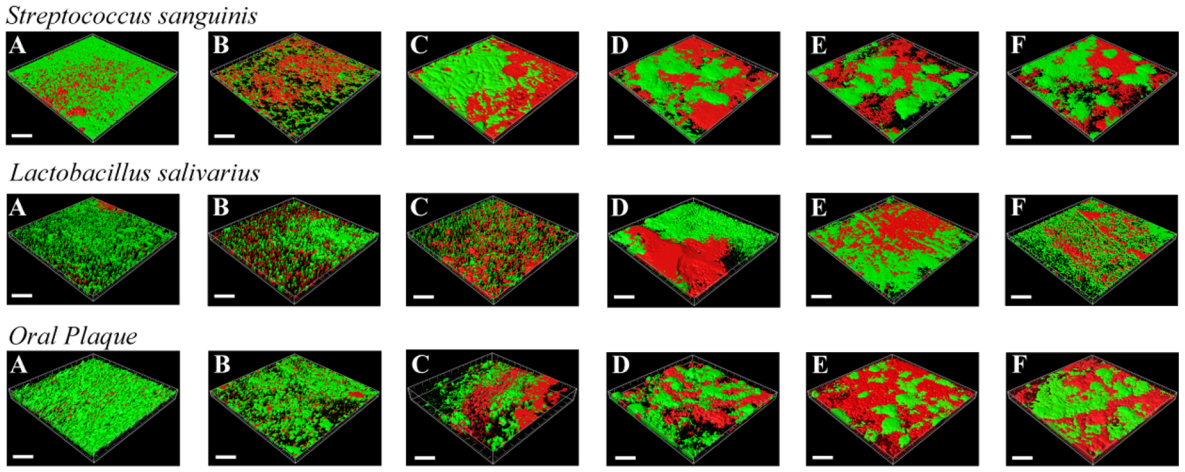

Figure 7. Live/dead staining of *S. sanguinis*, *L. salivarius*, and oral plaque after 4 weeks of incubation at 37 °C. (A) Ti, (B) Ti_Ag, (C) Ti_N_TSP, (D) Ti_N_CM_Lf, (E) Ti_ACoI_Lf, and (F) Ti_BCoI_Lf.

Organofunctional alkylsilanes have been widely used to form self-assembled monolayers on hydroxyl-terminated material surfaces in order to modify the properties or chemical functions of such surfaces. Moreover, silanes are commonly used for the immobilization of biomolecules.[20,40,47−49] The commonly used trialkoxysilane contains a silicon atom tetrahedrally coordinated to three similar hydrolyzable groups (such as methoxy or ethoxy groups) and to a functional group that introduces the desired chemical functionality, hence reactivity, to the substrate surface. In the present project, the use of two distinct organosilanes, TESPSA and CPTES, was studied. For both silanes, the silanization process is initialized by the activation of titanium surfaces by alkaline etching in order to generate hydroxyls groups onto titanium and to ensure an optimal silanization.[50] In previous studies, a reduction in bacteria adhesion and biofilm formation has been observed when TESPSA was attached onto titanium surfaces. Therefore, no antibacterial peptide has been conjugated onto TESPSA modified surfaces due to its antibacterial effects as has been previously reported. On the contrary, CPTES was used for AMP hLf1-11 immobilization. The synthetic hLf1-11 peptide showed antibacterial activity by binding to and altering the membrane of a broad range of bacteria[33,34,51,52] even when it was conjugated on titanium surfaces.[20,40]

ATRP methodology was developed as an alternative to the hLf1-11 immobilization method. The activation of titanium was performed by plasma activation, and the samples were modified with either APTES or BPTCS and followed by ATRP polymerization.[40] Interestingly, these two modifications differ in the reactive group of each silane. The amino group of APTES cannot initiate ATRP, thereby an additional step is necessary to activate it. Nevertheless, BPTCS contains bromide as a terminal group which already is an initiating species. Then, radicals are generated which periodically react with the transition metal complexes in their lower oxidation state. The effectiveness of the polymer brushes is a result of the immobilized peptide and the nonfouling properties of the PDMA segment.

4.1. Surface Characterization. Scanning electron microscopy (SEM) was used to observe the titanium surfaces after modification (Figure 2). It seems that the activation process has an important effect on morphology as the samples etched with NaOH showed a stable amorphous sodium titanate layer, with a characteristic nanoporous morphology (Figure 2B).[35] Contrary to this, plasma activation does not show any difference in comparison with smooth titanium (Figure 2A). Silver electrodeposition displayed round deposits which consist of silver,[17] and the rounded etching was a consequence of pretreatment which aimed at removing surface contamination and the native surface titanium oxide layer.[53]

The modifications observed in morphology are consistent with an increase in surface roughness in the treated samples (Table 2). Besides, kurtosis and skewness parameters[43] are influenced by the surface modification and suggested the effect in the sharpness of the peaks on the profile by silver deposition and ATRP polymerization. Noteworthy, surface roughness has an important impact in bacterial colonization because of the additional surface available for bacterial attachment.[54] However, in all the samples studied, the average roughness values (R_a) in the present study were below 0.2 μm, and on the basis of previous studies, it is not expected to significantly increase bacteria adhesion.[55]

In addition to surface roughness parameters, wettability was also examined. Wettability and SFE are relevant parameters determining chemical changes in surfaces and adhesion of cells and bacteria.[56−59] As shown in Table 1, the contact angles measured for treated surfaces did not show a drastic difference in comparison with control surfaces, with the exception of Ti_N_TSP. We expected that CPTES silanization, due to the hydrophobic nature of silane molecules, would have increased CA values. Moreover, copolymerization of DMA-*co*-APMA would have augmented the hydrophilic character of the samples due to the amides and amino groups introduced in the brushes. The results suggest that peptide immobilization varies the CA toward intermediate values of wettability, owing to its amphipathic character. Likewise, we believe that TESPSA silanization increased wettability values in comparison with activated titanium samples by NaOH treatment due to its hydrophobic character.

Some studies suggest a correlation between cellular adhesion and SFE on biomaterials.[60,61] They consider that values above the 20−30 mJ/m^2 range are optimal for cell adhesion.[62] In this regard, we expected that wettability of treated samples would show similar cellular adhesion.

The success in coating modifications in the present study was further measured by means of XPS studies (Table 3). Silver

DOI: 10.1021/acsami.5b00402
ACS Appl. Mater. Interfaces 2015, 7, 5992−6001

element was deposited onto titanium surfaces when the samples were electrochemically processed. For silanization and polymerization, an increase in the C 1S signal at high resolution was detected, which correlated with the presence of aliphatic carbons. This growth was accompanied by an increase in N 1s for peptide immobilization due to the amide and amino functionalities and other chemical groups characteristic of peptide molecules.[36,37] The presence of silicon was another indicator of silanization and sulfur for peptide attachment.

4.2. Biological Characterization of the Surfaces. Possible cytotoxic effects of treated surfaces were studied with adhesion and proliferation assays (Figures 3 and 4). The results did not reveal reduction in viable cells for up to 7 days of incubation. According to the International Organization for Standardization (ISO 10993-6:2007), reductions in cell viability of less than 20% are not considered cytotoxic. In addition, direct or indirect cytotoxic effects on HFFs were expected by the hLf1-11 peptide, TESPSA, and silver coatings methods used in this study, because of previous reports.[17,20,38,39] Once established that none of the treatments were cytotoxic, the study focused on the antimicrobial and/or antifouling properties against oral multispecies biofilm and the comparison of the effect on single species biofilm by two common oral bacteria, *S. sanguinis*[63,64] and *L. salivarius*.[11]

In this study, the effect of five different coatings was studied on bacterial adhesion and their ability to prevent or reduce biofilm formation. The entire modified surfaces have been previously tested using single-species biofilm. Oral biofilm, however, is an aggregation of multispecies bacteria. This fact raises some doubts on the validity of extending the results of *in vitro* studies with single-species biofilms to *in vivo* situations. Peri-implantitis is associated with more complex microbiota and greater diversity than periodontitis. It is composed of Gram-positive and Gram-negative bacteria and closely linked with primarily Gram-negative anaerobes, including *Porphyromonas gingivalis*, *Prevotella intermedia*, *Fusobacterium nucleatum*, and facultative *Aggregatibacter actinomycetemcomitans*.[65,66] Interestingly, previous studies have demonstrated that *in vitro* bacteria cultures of whole biofilms extracted from donors also reproduce the biofilm complexity found in *in vivo* oral biofilms, with the presence of multiple Gram-positive and Gram-negative bacteria.[5,65] However, therapeutic approaches for both diseases are similar.[67]

Is well-known that different antibacterial treatments differ in their efficacy against monospecies biofilms by different bacteria.[17,20,66] Therefore, development of *in vitro* multispecies oral plaque models are needed to achieve closer similarity with the *in vivo* oral and implant biofilms.[12−14]

The surface treated titanium samples displayed a promising reduction in bacterial adhesion (Figure 5). Overall, the results showed a reduction of biofilm on all modified surfaces, thus confirming the success of the coatings. Differences in the results between monospecies and multispecies biofilms emphasize the importance of developing further the multispecies plaque model.

Finally, the focus in the experiments was placed on the long-term antibacterial properties and biofilm formation onto modified coatings (Figures 6 and 7). These experiments showed that after 4 weeks of incubation the treated surfaces still showed a reduction in bacterial viability. Differences between the three biofilm types were again evident, exhibiting the same trend as obtained in the bacterial adhesion assay.

These results are of great interest because they demonstrate that distinct monospecies biofilms show differences in bacterial adhesion and long-term biofilm evolution. Besides, disparities are also obtained when oral plaque biofilm was used. Thus, bacterial strains exhibit different sensitivities to the activity of antibacterial and/or antifouling treatment.[66] Therefore, the use of monospecies biofilms should be discouraged as a model in implant-biofilm studies. In this regard, the *in vitro* multispecies oral biofilm method seems to be a preferred alternative to a monospecies methods.

The ratio of dead/live bacteria was also evaluated (Table 4). The fact that each strain and oral plaque has a distinct response to each antibacterial coating correlates with the results obtained in the bacterial viability assay. While Ti_Ag and Ti_N_TSP showed an increase in the proportion of dead cells through time, a dead/live decrease in Ti_N_CM_Lf, Ti_ACoI_Lf, and Ti_BCoI_Lf was detected only after 4 weeks of incubation.

The results of the present study showed that the antibacterial and/or antifouling coatings in the present study hold a great potential for dental applications. Differences have been detected when monospecies bacteria cultures and multispecies biofilm were studied *in vitro*.

5. CONCLUSIONS

Two different *in vitro* biofilm models were used to study the antibacterial properties of five different titanium surface coatings. The treated surfaces were physicochemically characterized in detail and were biocompatible with human fibroblasts. Both biofilm models demonstrated a drastic reduction in bacterial adhesion and a long-term effect on biofilm formation. A higher decrease was measured when a single-species bacteria model was used, especially for *S. sanguinis*. The *in vitro* multispecies biofilm model is a promising strategy to study the properties of antibacterial coatings because it more realistically mimics the complex microflora of peri-implantitis.

AUTHOR INFORMATION

Corresponding Author

*Phone: +34 934010711. Fax: +34 934016706. E-mail: daniel.rodriguez.rius@upc.edu.

Author Contributions

The manuscript was written through contributions of all authors. All authors have given approval to the final version of the manuscript.

Notes

The authors declare no competing financial interest.

ACKNOWLEDGMENTS

This study was supported by the Ministry of Economy and Competitiveness (MINECO) of the Spanish Government (Projects: MAT2009-12547, MAT2012-30706), Fundación Ramón Areces, and the European Union through European Regional Development Funds. Research reported in this study was also supported by the Canada Foundation for Innovation (CFI fund; Project No. 32623) and the National Natural Science Foundation of China (NSFC; Grant No. 81300904).

REFERENCES

(1) Algraffee, H.; Borumandi, F.; Cascarini, L. Peri-Implantitis. *Br. J. Oral Maxillofac. Surg.* **2012**, *50*, 689−694.

DOI: 10.1021/acsami.5b00402
ACS Appl. Mater. Interfaces 2015, 7, 5992−6001

(2) Klinge, B.; Hultin, M.; Berglundh, T. Peri-Implantitis. *Dent. Clin. North Am.* **2005**, *49*, 661−676 vii−viii..
(3) Foster, J. S.; Kolenbrander, P. E. Development of a Multispecies Oral Bacterial Community in a Saliva-Conditioned Flow Cell. *Appl. Environ. Microbiol.* **2004**, *70*, 4340−4348.
(4) Kolenbrander, P. E.; Andersen, R. N.; Blehert, D. S.; Egland, P. G.; Foster, J. S.; Palmer, R. J., Jr. Communication among Oral Bacteria. *Microbiol. Mol. Biol. Rev.* **2002**, *66*, 486−505.
(5) Sánchez, M. C.; Llama-Palacios, A.; Fernández, E.; Figuero, E.; Marín, M. J.; León, R.; Blanc, V.; Herrera, D.; Sanz, M. An *in Vitro* Biofilm Model Associated to Dental Implants: Structural and Quantitative Analysis of *in Vitro* Biofilm Formation on Different Dental Implant Surfaces. *Dent. Mater.* **2014**, *30*, 1161−1171.
(6) Benítez-Páez, A.; Belda-Ferre, P.; Simón-Soro, A.; Mira, A. Microbiota Diversity and Gene Expression Dynamics in Human Oral Biofilms. *BMC Genomics* **2014**, *15*, 311.
(7) Bjarnsholt, T. The Role of Bacterial Biofilms in Chronic Infections. *APMIS, Suppl.* **2013**, 1−51.
(8) Blanc, V.; Isabal, S.; Sánchez, M. C.; Llama-Palacios, A.; Herrera, D.; Sanz, M.; León, R. J. Characterization and Application of a Flow System for *in Vitro* Multispecies Oral Biofilm Formation. *Periodontal Res.* **2014**, *49*, 323−332.
(9) Takahashi, N. Microbial Ecosystem in the Oral Cavity: Metabolic Diversity in an Ecological Niche and Its Relationship with Oral Disease. *Int. Congr. Ser.* **2005**, *1284*, 103−112.
(10) Grössner-Schreiber, B.; Teichmann, J.; Hannig, M.; Dörfer, C.; Wenderoth, D. F.; Ott, S. J. Modified Implant Surfaces Show Different Biofilm Compositions under *in Vivo* Conditions. *Clin. Oral Implants Res.* **2009**, *20*, 817−826.
(11) Pham, L. C.; van Spanning, R. J. M.; Röling, W. F. M.; Prosperi, A. C.; Terefework, Z.; Ten Cate, J. M.; Crielaard, W.; Zaura, E. Effects of Probiotic *Lactobacillus salivarius* W24 on the Compositional Stability of Oral Microbial Communities. *Arch. Oral Biol.* **2009**, *54*, 132−137.
(12) Shen, Y.; Stojicic, S.; Haapasalo, M. Antimicrobial Efficacy of Chlorhexidine against Bacteria in Biofilms at Different Stages of Development. *J. Endod.* **2011**, *37*, 657−661.
(13) Shen, Y.; Stojicic, S.; Haapasalo, M. Bacterial Viability in Starved and Revitalized Biofilms: Comparison of Viability Staining and Direct Culture. *J. Endod.* **2010**, *36*, 1820−1823.
(14) Shen, Y.; Qian, W.; Chung, C.; Olsen, I.; Haapasalo, M. Evaluation of the Effect of Two Chlorhexidine Preparations on Biofilm Bacteria *in Vitro*: A Three-Dimensional Quantitative Analysis. *J. Endod.* **2009**, *35*, 981−985.
(15) Atiyeh, B. S.; Costagliola, M.; Hayek, S. N.; Dibo, S. A. Effect of Silver on Burn Wound Infection Control and Healing: Review of the Literature. *Burns J. Int. Soc. Burn Inj.* **2007**, *33*, 139−148.
(16) DeVasConCellos, P.; Bose, S.; Beyenal, H.; Bandyopadhyay, A.; Zirkle, L. G. Antimicrobial Particulate Silver Coatings on Stainless Steel Implants for Fracture Management. *Mater. Sci. Eng., C* **2012**, *32*, 1112−1120.
(17) Godoy-Gallardo, M.; Rodríguez-Hernández, A. G.; Delgado, L. M.; Manero, J. M.; Javier Gil, F.; Rodríguez, D. Silver Deposition on Titanium Surface by Electrochemical Anodizing Process Reduces Bacterial Adhesion of *Streptococcus sanguinis* and *Lactobacillus salivarius*. *Clin. Oral Implants Res.* **2014**, DOI: 10.1111/clr.12422.
(18) Brook, L. A.; Evans, P.; Foster, H. A.; Pemble, M. E.; Steele, A.; Sheel, D. W.; Yates, H. M. Highly Bioactive Silver and Silver/titania Composite Films Grown by Chemical Vapour Deposition. *J. Photochem. Photobiol. Chem.* **2007**, *187*, 53−63.
(19) Chen, W.; Liu, Y.; Courtney, H. S.; Bettenga, M.; Agrawal, C. M.; Bumgardner, J. D.; Ong, J. L. *In Vitro* Anti-Bacterial and Biological Properties of Magnetron Co-Sputtered Silver-Containing Hydroxyapatite Coating. *Biomaterials* **2006**, *27*, 5512−5517.
(20) Godoy-Gallardo, M.; Mas-Moruno, C.; Fernández-Calderón, M. C.; Pérez-Giraldo, C.; Manero, J. M.; Albericio, F.; Gil, F. J.; Rodríguez, D. Covalent Immobilization of hLf1-11 Peptide on a Titanium Surface Reduces Bacterial Adhesion and Biofilm Formation. *Acta Biomater.* **2014**, *10*, 3522−3534.
(21) Chen, X.; Sevilla, P.; Aparicio, C. Surface Biofunctionalization by Covalent Co-Immobilization of Oligopeptides. *Colloids Surf., B: Biointerfaces* **2013**, *107*, 189−197.
(22) Li, X.; Li, P.; Saravanan, R.; Basu, A.; Mishra, B.; Lim, S. H.; Su, X.; Tambyah, P. A.; Leong, S. S. J. Antimicrobial Functionalization of Silicone Surfaces with Engineered Short Peptides Having Broad Spectrum Antimicrobial and Salt-Resistant Properties. *Acta Biomater.* **2014**, *10*, 258−266.
(23) Xie, Y.; Hill, C. A. S.; Xiao, Z.; Militz, H.; Mai, C. Silane Coupling Agents Used for Natural Fiber/polymer Composites: A Review. *Composites, Part A: Appl. Sci. Manuf.* **2010**, *41*, 806−819.
(24) Bauer, S.; Schmuki, P.; von der Mark, K.; Park, J. Engineering Biocompatible Implant Surfaces: Part I: Materials and Surfaces. *Prog. Mater. Sci.* **2013**, *58*, 261−326.
(25) Ahmed, W.; Subramani, K. *Emerging Nanotechnologies in Dentistry: Materials, Processes, and Applications*; William Andrew: Waltham, MA, 2012.
(26) Costa, F.; Carvalho, I. F.; Montelaro, R. C.; Gomes, P.; Martins, M. C. L. Covalent Immobilization of Antimicrobial Peptides (AMPs) onto Biomaterial Surfaces. *Acta Biomater.* **2011**, *7*, 1431−1440.
(27) Onaizi, S. A.; Leong, S. S. J. Tethering Antimicrobial Peptides: Current Status and Potential Challenges. *Biotechnol. Adv.* **2011**, *29*, 67−74.
(28) Holmberg, K. V.; Abdolhosseini, M.; Li, Y.; Chen, X.; Gorr, S.-U.; Aparicio, C. Bio-Inspired Stable Antimicrobial Peptide Coatings for Dental Applications. *Acta Biomater.* **2013**, *9*, 8224−8231.
(29) Chen, R.; Willcox, M. D. P.; Cole, N.; Ho, K. K. K.; Rasul, R.; Denman, J. A.; Kumar, N. Characterization of Chemoselective Surface Attachment of the Cationic Peptide Melimine and Its Effects on Antimicrobial Activity. *Acta Biomater.* **2012**, *8*, 4371−4379.
(30) Pasupuleti, M.; Schmidtchen, A.; Malmsten, M. Antimicrobial Peptides: Key Components of the Innate Immune System. *Crit. Rev. Biotechnol.* **2012**, *32*, 143−171.
(31) Reddy, K. V. R.; Yedery, R. D.; Aranha, C. Antimicrobial Peptides: Premises and Promises. *Int. J. Antimicrob. Agents* **2004**, *24*, 536−547.
(32) Bouchet, A. M.; Iannucci, N. B.; Pastrian, M. B.; Cascone, O.; Santos, N. C.; Disalvo, E. A.; Hollmann, A. Biological Activity of Antibacterial Peptides Matches Synergism between Electrostatic and Non Electrostatic Forces. *Colloids Surf., B: Biointerfaces* **2014**, *114*, 363−371.
(33) Jenssen, H.; Hancock, R. E. W. Antimicrobial Properties of Lactoferrin. *Biochimie* **2009**, *91*, 19−29.
(34) Kirkpatrick, C. H.; Green, I.; Rich, R. R.; Schade, A. L. Inhibition of Growth of *Candida albicans* by Iron-Unsaturated Lactoferrin: Relation to Host-Defense Mechanisms in Chronic Mucocutaneous Candidiasis. *J. Infect. Dis.* **1971**, *124*, 539−544.
(35) Kim, H. M.; Miyaji, F.; Kokubo, T.; Nakamura, T. Effect of Heat Treatment on Apatite-Forming Ability of Ti Metal Induced by Alkali Treatment. *J. Mater. Sci. Mater. Med.* **1997**, *8*, 341−347.
(36) Xiao, S. J.; Textor, M.; Spencer, N. D.; Wieland, M.; Keller, B.; Sigrist, H. Immobilization of the Cell-Adhesive Peptide Arg-Gly-Asp-Cys (RGDC) on Titanium Surfaces by Covalent Chemical Attachment. *J. Mater. Sci. Mater. Med.* **1997**, *8*, 867−872.
(37) Xiao, S.-J.; Textor, M.; Spencer, N. D.; Sigrist, H. Covalent Attachment of Cell-Adhesive, (Arg-Gly-Asp)-Containing Peptides to Titanium Surfaces. *Langmuir* **1998**, *14*, 5507−5516.
(38) Gao, G.; Yu, K.; Kindrachuk, J.; Brooks, D. E.; Hancock, R. E. W.; Kizhakkedathu, J. N. Antibacterial Surfaces Based on Polymer Brushes: Investigation on the Influence of Brush Properties on Antimicrobial Peptide Immobilization and Antimicrobial Activity. *Biomacromolecules* **2011**, *12*, 3715−3727.
(39) Gao, G.; Lange, D.; Hilpert, K.; Kindrachuk, J.; Zou, Y.; Cheng, J. T. J.; Kazemzadeh-Narbat, M.; Yu, K.; Wang, R.; Straus, S. K.; Brooks, D. E.; Chew, B. H.; Hancock, R. E. W.; Kizhakkedathu, J. N. The Biocompatibility and Biofilm Resistance of Implant Coatings Based on Hydrophilic Polymer Brushes Conjugated with Antimicrobial Peptides. *Biomaterials* **2011**, *32*, 3899−3909.

DOI: 10.1021/acsami.5b00402
ACS Appl. Mater. Interfaces 2015, 7, 5992−6001

(40) Godoy-Gallardo, M.; Mas-Moruno, C.; Yu, K.; Manero, J. M.; Gil, F. J.; Kizhakkedathu, J. N.; Rodriguez, D. Antibacterial Properties of hLf1-11 Peptide onto Titanium Surfaces: A Comparison Study Between Silanization and Surface Initiated Polymerization. *Biomacromolecules* **2014**, *16*, 483−496.
(41) Matyjaszewski, K.; Miller, P. J.; Shukla, N.; Immaraporn, B.; Gelman, A.; Luokala, B. B.; Siclovan, T. M.; Kickelbick, G.; Vallant, T.; Hoffmann, H.; Pakula, T. Polymers at Interfaces: Using Atom Transfer Radical Polymerization in the Controlled Growth of Homopolymers and Block Copolymers from Silicon Surfaces in the Absence of Untethered Sacrificial Initiator. *Macromolecules* **1999**, *32*, 8716−8724.
(42) Peltonen, J.; Järn, M.; Areva, S.; Linden, M.; Rosenholm, J. B. Topographical Parameters for Specifying a Three-Dimensional Surface. *Langmuir* **2004**, *20*, 9428−9431.
(43) Gadelmawla, E. S.; Koura, M. M.; Maksoud, T. M. A.; Elewa, I. M.; Soliman, H. H. Roughness Parameters. *J. Mater. Process. Technol.* **2002**, *123*, 133−145.
(44) Aparicio, C.; Padrós, A.; Gil, F.-J. *In Vivo* Evaluation of Micro-Rough and Bioactive Titanium Dental Implants Using Histometry and Pull-out Tests. *J. Mech. Behav. Biomed. Mater.* **2011**, *4*, 1672−1682.
(45) Zhao, L.; Chu, P. K.; Zhang, Y.; Wu, Z. Antibacterial Coatings on Titanium Implants. *J. Biomed. Mater. Res., Part B: Appl. Biomater.* **2009**, *91B*, 470−480.
(46) Kim, J.; Pitts, B.; Stewart, P. S.; Camper, A.; Yoon, J. Comparison of the Antimicrobial Effects of Chlorine, Silver Ion, and Tobramycin on Biofilm. *Antimicrob. Agents Chemother.* **2008**, *52*, 1446−1453.
(47) Shriver-Lake, L. C.; Donner, B.; Edelstein, R.; Breslin, K.; Bhatia, S. K.; Ligler, F. S. Antibody Immobilization Using Heterobifunctional Crosslinkers. *Biosens. Bioelectron.* **1997**, *12*, 1101−1106.
(48) Chen, W.-C.; Ko, C.-L. Roughened Titanium Surfaces with Silane and Further RGD Peptide Modification *in Vitro*. *Mater. Sci. Eng., C* **2013**, *33*, 2713−2722.
(49) Guha Thakurta, S.; Subramanian, A. Fabrication of Dense, Uniform Aminosilane Monolayers: A Platform for Protein or Ligand Immobilization. *Colloids Surf., A: Physicochem. Eng. Aspects* **2012**, *414*, 384−392.
(50) Han, Y.; Mayer, D.; Offenhäusser, A.; Ingebrandt, S. Surface Activation of Thin Silicon Oxides by Wet Cleaning and Silanization. *Thin Solid Films* **2006**, *510*, 175−180.
(51) Bellamy, W.; Takase, M.; Wakabayashi, H.; Kawase, K.; Tomita, M. Antibacterial Spectrum of Lactoferricin B, a Potent Bactericidal Peptide Derived from the N-Terminal Region of Bovine Lactoferrin. *J. Appl. Bacteriol.* **1992**, *73*, 472−479.
(52) Brouwer, C. P. J. M.; Rahman, M.; Welling, M. M. Discovery and Development of a Synthetic Peptide Derived from Lactoferrin for Clinical Use. *Peptides* **2011**, *32*, 1953−1963.
(53) Vermesse, E.; Mabru, C.; Arurault, L. Surface Integrity after Pickling and Anodization of Ti−6Al−4V Titanium Alloy. *Appl. Surf. Sci.* **2013**, *285*, 629−637.
(54) Rodríguez-Hernández, A.; Espinar, E.; Llamas, J. M.; Barrera, J. M.; Gil, F. J. Alumina Shot-Blasted Particles on Commercially Pure Titanium Surfaces Prevent Bacterial Attachment. *Mater. Lett.* **2013**, *92*, 42−44.
(55) Barbour, M. E.; O'Sullivan, D. J.; Jenkinson, H. F.; Jagger, D. C. The Effects of Polishing Methods on Surface Morphology, Roughness and Bacterial Colonisation of Titanium Abutments. *J. Mater. Sci. Mater. Med.* **2007**, *18*, 1439−1447.
(56) Rupp, F.; Gittens, R. A.; Scheideler, L.; Marmur, A.; Boyan, B. D.; Schwartz, Z.; Geis-Gerstorfer, J. A Review on the Wettability of Dental Implant Surfaces I: Theoretical and Experimental Aspects. *Acta Biomater.* **2014**, *10*, 2894−2906.
(57) Tzoneva, R.; Faucheux, N.; Groth, T. Wettability of Substrata Controls Cell−Substrate and Cell−Cell Adhesions. *Biochim. Biophys. Acta, Gen. Subj.* **2007**, *1770*, 1538−1547.
(58) Amoroso, P. F.; Pier-Francesco, A.; Adams, R. J.; Waters, M. G. J.; Williams, D. W. Titanium Surface Modification and Its Effect on the Adherence of Porphyromonas Gingivalis: An *in Vitro* Study. *Clin. Oral Implants Res.* **2006**, *17*, 633−637.
(59) Dexter, S. C. Influence of Substratum Critical Surface Tension on Bacterial Adhesion—in Situ Studies. *J. Colloid Interface Sci.* **1979**, *70*, 346−354.
(60) Harnett, E. M.; Alderman, J.; Wood, T. The Surface Energy of Various Biomaterials Coated with Adhesion Molecules Used in Cell Culture. *Colloids Surf., B: Biointerfaces* **2007**, *55*, 90−97.
(61) Bacakova, L.; Filova, E.; Parizek, M.; Ruml, T.; Svorcik, V. Modulation of Cell Adhesion, Proliferation and Differentiation on Materials Designed for Body Implants. *Biotechnol. Adv.* **2011**, *29*, 739−767.
(62) Pegueroles, M.; Gil, F. J.; Planell, J. A.; Aparicio, C. The Influence of Blasting and Sterilization on Static and Time-Related Wettability and Surface-Energy Properties of Titanium Surfaces. *Surf. Coat. Technol.* **2008**, *202*, 3470−3479.
(63) Kolenbrander, P. E.; Andersen, R. N.; Moore, L. V. Intrageneric Coaggregation among Strains of Human Oral Bacteria: Potential Role in Primary Colonization of the Tooth Surface. *Appl. Environ. Microbiol.* **1990**, *56*, 3890−3894.
(64) Rickard, A. H.; McBain, A. J.; Ledder, R. G.; Handley, P. S.; Gilbert, P. Coaggregation between Freshwater Bacteria within Biofilm and Planktonic Communities. *FEMS Microbiol. Lett.* **2003**, *220*, 133−140.
(65) Charalampakis, G.; Rabe, P.; Leonhardt, A.; Dahlén, G. A Follow-up Study of Peri-Implantitis Cases after Treatment. *J. Clin. Periodontol.* **2011**, *38*, 864−871.
(66) Goudouri, O.-M.; Kontonasaki, E.; Lohbauer, U.; Boccaccini, A. R. Antibacterial Properties of Metal and Metalloid Ions in Chronic Periodontitis and Peri-Implantitis Therapy. *Acta Biomater.* **2014**, *10*, 3795−3810.
(67) D'Ercole, S.; Piattelli, A.; Marzo, G.; Scarano, A.; Tripodi, D. Influence of Bacterial Colonization of the Healing Screws on Peri-Implant Tissue. *J. Dent. Sci.* **2013**, *8*, 109−114.

DOI: 10.1021/acsami.5b00402
ACS Appl. Mater. Interfaces 2015, 7, 5992−6001